European Heart Journal (2008) **29**, 2148–2155
doi:10.1093/eurheartj/ehn297

High spatial resolution myocardial perfusion cardiac magnetic resonance for the detection of coronary artery disease

Sven Plein[1,2]*, Sebastian Kozerke[1], Daniel Suerder[3], Thomas F. Luescher[3], John P. Greenwood[2], Peter Boesiger[1], and Juerg Schwitter[3]

[1]Institute for Biomedical Engineering, University and ETH Zurich, Zurich, Switzerland; [2]Academic Unit of Cardiovascular Medicine, University of Leeds, G-Floor Jubilee Wing, Leeds General Infirmary, Great George Street, Leeds LS1 3EX, UK; and [3]Cardiovascular Centre, Department of Cardiology, University Hospital Zurich, Zurich, Switzerland

Received 28 January 2008; revised 5 June 2008; accepted 11 June 2008; online publish-ahead-of-print 18 July 2008

Aims To evaluate the feasibility and diagnostic performance of high spatial resolution myocardial perfusion cardiac magnetic resonance (perfusion-CMR).

Methods and results Fifty-four patients underwent adenosine stress perfusion-CMR. An in-plane spatial resolution of 1.4 × 1.4 mm^2 was achieved by using 5× *k*-space and time sensitivity encoding (*k*–*t* SENSE). Perfusion was visually graded for 16 left ventricular and two right ventricular (RV) segments on a scale from 0 = normal to 3 = abnormal, yielding a perfusion score of 0–54. Diagnostic accuracy of the perfusion score to detect coronary artery stenosis of >50% on quantitative coronary angiography was determined. Sources and extent of image artefacts were documented.

Two studies (4%) were non-diagnostic because of *k*–*t* SENSE-related and breathing artefacts. Endocardial dark rim artefacts if present were small (average width 1.6 mm). Analysis by receiver–operating characteristics yielded an area under the curve for detection of coronary stenosis of 0.85 [95% confidence interval (CI) 0.75–0.95] for all patients and 0.82 (95% CI 0.65–0.94) and 0.87 (95% CI 0.75–0.99) for patients with single and multi-vessel disease, respectively. Seventy-four of 102 (72%) RV segments could be analysed.

Conclusion High spatial resolution perfusion-CMR is feasible in a clinical population, yields high accuracy to detect single and multi-vessel coronary artery disease, minimizes artefacts and may permit the assessment of RV perfusion.

Keywords Magnetic resonance imaging • Myocardial perfusion • Ischaemia • Coronary artery disease

Introduction

The use of first-pass myocardial perfusion cardiac magnetic resonance (perfusion-CMR) to detect left ventricular (LV) ischaemia has been extensively validated.[1–5] Combined with an assessment of ventricular function by cine imaging and viability by late gadolinium enhancement (late-gadolinium-enhanced-CMR; LGE-CMR), perfusion-CMR allows for a comprehensive assessment of coronary artery disease (CAD).[6,7] However, currently perfusion-CMR yields a substantially lower spatial resolution than these other CMR methods.[1–11] The main reason for this limitation is that in a first-pass perfusion-CMR study all data have to be acquired in a single shot in a limited portion of each cardiac cycle. Acquisition of cine and LGE-CMR data on the other hand can be segmented and acquired over several heartbeats to boost spatial resolution and/or signal-to-noise ratio.

New acquisition strategies such as *k*-space and time sensitivity encoding (*k*–*t* SENSE), that simultaneously exploit coil encoding and spatiotemporal correlations, allow substantial acceleration of CMR data acquisition.[12,13] This speed-up can be utilized to

* Corresponding author. Tel: +44 113 392 5404, Fax: +44 113 392 5405, Email: s.plein@leeds.ac.uk

either improve spatial resolution, shorten acquisition time per slice or increase signal-to-noise ratio. The feasibility of high spatial resolution *k–t* SENSE accelerated perfusion-CMR has been demonstrated in principle in volunteers.[14] In clinical application, the high spatial resolution should have several benefits, including: (i) better integration of perfusion with cine and LGE-CMR data, (ii) minimal impact of endocardial dark-banding artefacts, which will be reduced in extent according to the smaller voxel size, and (iii) assessment of the transmural distribution of ischaemia in several myocardial layers. Potentially, the high spatial resolution may also permit the assessment of perfusion of the thin-walled right ventricular (RV) myocardium, previously not measurable by perfusion-CMR.

The purpose of this study was to assess the feasibility of high spatial resolution perfusion-CMR for clinical application and to determine its diagnostic accuracy to detect ischaemia of the left and right ventricle and in multi-vessel disease.

Methods

Patients

Patients awaiting diagnostic invasive X-ray coronary angiography for evaluation of known or suspected CAD were included in the study. Exclusion criteria were contraindications to CMR (cardiac magnetic resonance) (incompatible metallic implants, claustrophobia) or adenosine infusion (asthma, AV block), myocardial infarction within 7 days, unstable angina pectoris and NYHA Class 4 heart failure. Over a predefined period of 6 months, all patients fulfilling the inclusion criteria were prospectively identified and contacted. Recruitment ended after 6 months. Out of 136 suitable patients identified in the recruitment period, 82 declined participation so that 54 patients (42 male, mean age 59 years, range 39–79) were eventually recruited. All recruited patients completed the study. Patients were instructed to refrain from substances containing caffeine for 24 h before the examination. Cardiac medication was not stopped prior to CMR. All patients gave written informed consent and the study was approved by the local ethics review board.

Cardiac magnetic resonance

CMR studies were carried out on a clinical 1.5T MR system (Philips Medical Systems, Best, The Netherlands) using a five-element cardiac phased array receiver coil for signal reception. All CMR data were acquired in the true short axis of the LV, and in contrast to many previous CMR studies, data were acquired in end-inspiration. This approach was chosen to maximize the breath-hold capacity of the patients.

Adenosine was administered intravenously at a dose of 140 μg/kg/min under continuous heart rate and blood pressure monitoring at 1 min intervals. After 3 min of the adenosine infusion, an intravenous bolus injection of 0.1 mmol/kg Gadobutrolum (Gadovist, Schering, Berlin, Germany) was administered into an antecubital vein on the opposing arm with the use of a power injector (Medrad Spectris Solaris, Medrad, Indianola, PA, USA; injection rate 5 mL/s followed by a 20 mL Saline flush at 5 mL/s). The pulse sequence used for perfusion-CMR has been described in detail elsewhere.[14] In brief, a saturation recovery gradient echo pulse sequence accelerated with *k–t* SENSE was used with a repetition time of 3.1 ms, echo time of 1.1 ms, flip angle 15°, acquisition window 120 ms, spatial resolution matched to cine and LGE-CMR at $1.4 \times 1.4 \times 10\ mm^3$. The *k–t* SENSE acceleration factor was five with 11 training profiles acquired interleaved with the undersampled data. In order to sample data in cardiac phases with minimal bulk cardiac motion and minimize motion-related artefacts, acquisition was limited to four short-axis sections acquired at alternate heartbeats. To achieve this, mid-systole and mid-diastole were identified on cine images and the trigger delays for the perfusion acquisition set so that acquisition occurred in these cardiac phases. The dynamic scan duration for the perfusion study was adjusted to the breath-hold capability of each individual as determined by non-contrast enhanced test scans.

In all patients cine and LGE-CMR was also performed in identical slice orientations and during inspiratory breath-holding using conventional methods (spatial resolution $1.4 \times 1.4 \times 10\ mm^3$).

Cardiac magnetic resonance analysis

All data were reviewed on a post-processing workstation (Viewforum, Philips Medical Systems, Best, The Netherlands) by an expert observer with >5 years experience in reading >100 perfusion-CMR studies per year. The observer was blinded to all clinical information. For assessment of observer variability, a second expert (3 years experience in reading >100 perfusion-CMR studies per year) independently repeated the analysis.

Image quality was graded on a scale between 0 and 3 (0 = non-diagnostic, 1 = poor, 2 = good, 3 = excellent). Occurrence of artefacts related to the *k–t* reconstruction, respiratory motion, and endocardial dark banding were recorded. It was further noted whether *k–t* reconstruction-related and motion artefacts affected the first myocardial contrast passage. Dark-banding artefacts were recorded if an endocardial dark band appeared at the arrival of contrast in the LV cavity and prior to contrast arrival in the myocardium. The maximal transmural width of endocardial dark-banding artefacts was measured using electronic callipers.

Visual perfusion analysis used 16 segments of the AHA (American Heart Association) model for LV assessment.[15] The two middle sections of the perfusion-CMR studies were combined to yield segments 7–12 (mid-ventricular level) of the model. In addition, perfusion of the RV free wall was assessed for two RV segments (anterior and inferior), yielding a total of 18 segments per patient. Perfusion in a segment was considered abnormal if:

- signal enhancement was reduced compared with remote myocardial segments; or
- an endocardial to epicardial perfusion gradient within a segment was present; and
- if the perfusion defect was not located within scar tissue on corresponding LGE-CMR images.

Stress perfusion in each segment was scored on a scale from 0 to 3 (0 = normal, 1 = probably normal, 2 = probably abnormal or subendocardial defect, 3 = abnormal or transmural defect). By summing all segmental scores, a perfusion score of 0–54 was calculated for each patient. Separate perfusion scores were calculated for the left anterior descending (LAD), circumflex (Cx), and right coronary artery (RCA) territories according to the AHA segmentation.[15] For this, the inferior RV segment was added to the RCA perfusion score and the anterior RV segment to the LAD score.

X-ray coronary angiography

Following the CMR examination, all patients underwent biplane coronary angiography using a standard technique. Angiograms were analysed by quantitative coronary analysis (QCA) (Xelera 1.2 L4 SP1, Philips Medical Systems, Best, The Netherlands) by an independent blinded reviewer. Coronary lesions were analysed

in several projections. The outer diameter of the contrast-filled guiding catheter was used for calibration. The severity of any coronary lesion was evaluated measuring minimal lumen diameter and per cent diameter stenosis in several angiographic views. The most severe stenosis was recorded. For analysis purposes, only vessels with a reference diameter of >2 mm were included. Based on these analyses, patients were classified as having one-, two-, or three-vessel disease.

Statistical analysis

Statistical analysis used Analyse-it software (Analyse-it, Leeds, UK). Continuous data were expressed as the mean ± SD and comparisons between groups were made using two-sided paired *t*-test for continuous data. Discrete data were expressed as percentages. Statistical significance was considered for $P < 0.05$.

Receiver operating characteristic (ROC) analyses were performed to evaluate the diagnostic performance of the perfusion score to detect coronary stenosis of >50% on QCA.[16] In addition to this primary analysis, the stenosis severities >70% and >75%, which have been used in previous studies, were also analysed. Areas under the curve (AUCs) with 95% confidence intervals (95% CI) were determined from ROC analysis. Agreement between observers for the overall perfusion scores was assessed using the method described by Bland and Altman.[17]

Results

All studies were completed. Data from one subject was not available for analysis because of a reconstruction error. Both observers scored one additional study as non-diagnostic because of a combination of ECG gating and respiratory motion artefacts and one observer excluded another patient on the basis of poor image quality. Fifty-one patients (94%) were thus available for the final analysis. Clinical details of the study group are given in *Table 1*.

Cardiac magnetic resonance imaging

Forty patients experienced side effects during the adenosine infusion (breathlessness, flushing, headache), but no clinically relevant complications occurred. Heart rate increased from 64 ± 9 to 74 ± 8 b.p.m. ($P = 0.0001$) during stress, while systolic blood pressure did not change significantly during adenosine infusion (124 ± 12 to 122 ± 14 mmHg, $P = 0.26$).

Coronary angiography

X-ray angiography was carried out at a median of 4 days (interquartile range 6) of the CMR study. Of the 51 patients included in the final analysis, 16 (31%) had no coronary artery stenosis of >50%. Fourteen patients (27%) had one-vessel disease, 17 (33%) two-vessel disease, three (6%) had three-vessel disease and one patient (2%) had significant left main stem stenosis. *Table 1* lists further details of the angiographic characteristics of the study group.

Diagnostic accuracy

Mean perfusion score was 8 (95% CI 6–10), with a median of 6.5 (95% CI 3–10), a range of 29 and an interquartile range of 11.25.

Table 1 Base-line demographic characteristics, cardiac risk factors and angiographic findings of patients included in the analysis ($n = 51$)

Sex, *n* (%)	
Male	39 (76%)
Female	12 (24%)
Age (years)[a]	59 (±10)
Risk factors, *n* (%)	
Diabetes mellitus	7 (14%)
Hypertension	35 (68%)
Hypercholesterolaemia	36 (70%)
Previous MI	6 (12%)
Previous PCI	4 (8%)
Smoker	29 (57%)
Angiography findings	
No significant disease[b]	16 (31%)
One-vessel disease[b]	14 (27%)
Two-vessel disease[b]	17 (33%)
Three-vessel disease[b]	3 (6%)
Left main stem disease[b]	1 (2%)
LAD disease[b]	20 (39%)
Cx disease[b]	17 (33%)
RCA disease[b]	22 (43%)

PCI, percutaneous coronary intervention; MI, myocardial infarction; LAD, left anterior descending artery; Cx, circumflex artery; RCA, right coronary artery.
[a]Plus/minus values are mean ± SD.
[b]Coronary stenosis > 50% on QCA (quantitative coronary analysis).

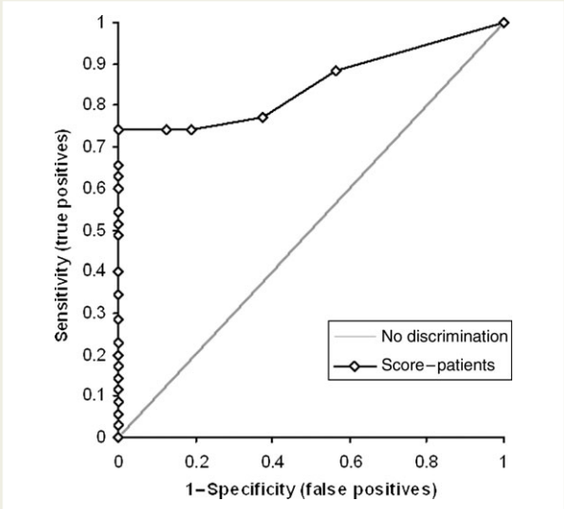

Figure 1 Receiver–operating characteristics curve for the ability of the cardiac magnetic resonance perfusion score to detect coronary artery disease >50%.

The AUC of the ROC analysis for the ability of the CMR perfusion score to detect the presence of coronary disease >50% was 0.85 (95% CI 0.75–0.95) (*Figure 1*). Diagnostic performance was

Table 2 Areas under the receiver–operating characteristics curves and 95% confidence interval (CI) for the detection of coronary stenosis at different disease severities and disease extent. Given in brackets are the numbers of patients with one or multi-vessel disease at the three disease severity cut-offs

	>50%	>70%	>75%
One-vessel disease	0.82 (0.70–0.94) ($n = 14$)	0.81 (0.70–0.92) ($n = 14$)	0.87 (0.75–0.99) ($n = 14$)
Multi-vessel disease	0.87 (0.75–0.99) ($n = 21$)	0.86 (0.73–0.99) ($n = 18$)	0.81 (0.68–0.94) ($n = 14$)

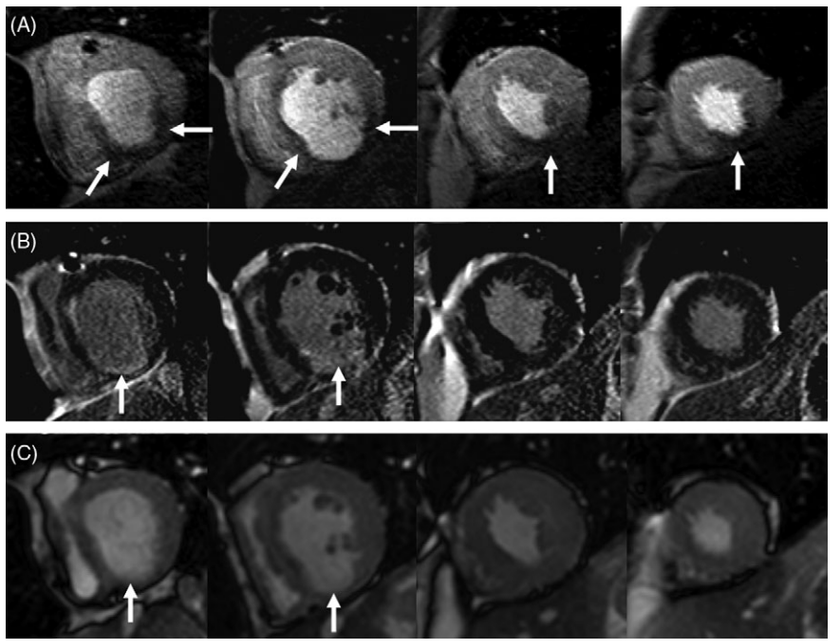

Figure 2 Case example: 47-year-old male with previous inferior myocardial infarction, in whom subsequent coronary angiography showed chronic total occlusion of the right coronary artery and a patent proximal left anterior descending artery stent. The top row shows adenosine stress myocardial perfusion images at peak myocardial contrast enhancement, the middle row the corresponding late-gadolinium enhanced images and the bottom row matching frames from the cine data sets. An infero-basal scar with thinning of the myocardium can be seen in all images. Perfusion images show peri-infarct ischaemia extending circumferentially outside the scar at the basal level (arrows). In addition, there is ischaemia in the viable apical inferior segments. The correlation of the cardiac magnetic resonance components is facilitated by their identical orientation and spatial resolution.

unchanged if the six patients with a history of MI were excluded from the analysis. Similar diagnostic performance was seen at coronary stenosis levels of >70 and >75% (AUC 0.83, 95% CI 0.71–0.95 and 0.84, 95% CI 0.73–0.95, respectively). Diagnostic accuracy was similar for single and multi-vessel (two- or three-vessel) disease (at disease severity >50%: AUC 0.82, 95% CI 0.70–0.94 vs. 0.87, 95% CI 0.75–0.99, respectively). *Table 2* lists all results of one-vessel and multi-vessel disease at different disease severities.

AUC of the ROC analysis were 0.78 (95% CI 0.64–0.94), 0.82 (95% CI 0.68–0.96), and 0.80 (95% CI 0.66–0.94) for the detection of >50% coronary stenosis in the LAD, Cx, and RCA, respectively.

Correlation with other cardiac magnetic resonance components

In one half (three of six) of the patients with previous myocardial infarction, peri-infarct ischaemia was demonstrated by perfusion-CMR. An example is shown in *Figure 2* from a patient with previous inferior myocardial infarction, chronic total occlusion of the RCA, and ongoing angina following elective percutaneous intervention to the proximal LAD. LGE-CMR images demonstrated an inferior scar at mid-ventricular and basal levels with corresponding wall motion abnormalities on cine imaging. Perfusion-CMR identified inferior peri-infarct ischaemia in viable myocardium around the scar. No ischaemia was seen in the LAD territory. The patient's symptoms

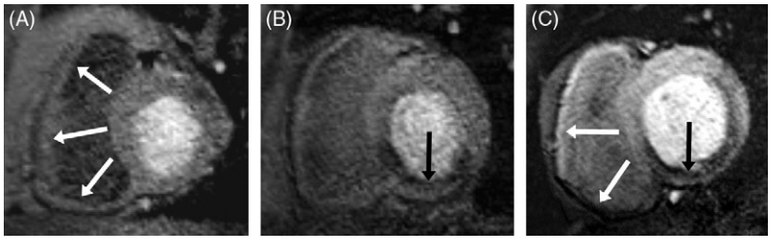

Figure 3 Case examples of right ventricular (RV) perfusion. Images from perfusion-cardiac magnetic resonance of three patients. Only one slice of the four acquired sections and only the dynamic image with the clearest contrast between RV free wall and blood pool are shown. (*A*) Normal RV perfusion in a patient with a normal right coronary artery (RCA) and left anterior descend artery (white arrows). (*B*) Normal RV perfusion is seen in a patient with a mid-RCA lesion and ischaemia in the inferior segment of the left ventricle (LV) (black arrow) due to a mid-vessel occlusion of the RCA. (*C*) Inferior RV (white arrows) and LV (black arrow) ischaemia can be seen in a patient with a proximal RCA stenosis. The white arrows point to high signal in the anterior RV wall and low signal in the inferior RV wall, suggesting reduced perfusion in the RV inferior segment, which is most evident when compared with normal inferior RV perfusion in the examples shown in (*A*) and (*B*).

were thus assumed to be caused by peri-infarct ischaemia in the RCA territory. Subsequent invasive angiography confirmed the chronic occlusion of the RCA and a patent LAD stent. An attempt to open the RCA occlusion failed.

Right ventricular perfusion

Seventy-four of 102 (72%) of RV segments could be analysed. In the remaining segments the RV free wall could not be clearly differentiated from blood pool or extra-cardiac tissue during the first pass of the contrast agent. In five patients RV ischaemia was detected and was specific for proximal RCA disease (five out of five). *Figure 3A* shows normal RV perfusion in a patient with normal RCA and LAD, *Figure 3B* normal RV perfusion in a patient with a mid-RCA lesion, and *Figure 3C* inferior RV ischaemia in a patient with a proximal RCA stenosis.

Image quality and artefacts

Figure 4 illustrates the dynamic transmural redistribution of blood flow during the first pass of the contrast passage in a patient with a stenosis in the proximal LAD (90% on QCA). In *Figure 4A* and *B* images acquired in the early part of the myocardial contrast passage reveal a transmural perfusion defect which becomes subendocardial in the later stages of the contrast passage in *Figure 4C* and *D*.

The mean image quality score was 1.9. Dark-banding artefacts were seen in 25 data sets, but were limited to the endocardial border of diastolic images and measured on average 1.6 mm in width. There were no cases in which dark-banding artefacts were reported as significant. A typical dark-banding artefact can be seen in the most basal slice of *Figure 4A*. Five data sets were affected by *k*–*t* reconstruction artefacts, all in patients who were unable to hold their breath for the duration of the scan (*Figure 5*). Two of these studies were excluded from the analysis because artefacts affected the myocardial contrast passage, while in the other three the myocardial contrast passage was unaffected by the artefacts.

Interobserver agreement

Out of 816 segments analysed, the observers awarded the same segmental perfusion score in 650 (79.8%). The same score or one grade difference was given for 756 segments (92.8%). Agreement analysis for the overall perfusion score showed a mean bias of −0.8 with 95% limits of agreement of −11.8 (95% CI −14.5 to −9.0) to 10.2 (95% CI 7.5–12.9). Image quality scores were similar between both observers (1.9 vs. 1.8, $P = 0.12$) with a one-grade difference in six patients. AUC of the ROC analysis were similar for the main analysis of coronary stenosis >50%: 0.85 (95% CI 0.75–0.95) vs. 0.83 (95% CI 0.72–0.94), $P = 0.75$.

Discussion

This study shows that stress perfusion-CMR at high spatial resolution, facilitated by *k*–*t* SENSE acceleration, can be applied to a clinical population with suspected CAD. Visual analysis of the data provides high diagnostic accuracy for the detection of coronary stenosis in single and multi-vessel disease. The high spatial resolution facilitates an integrated analysis of perfusion, cine, and LGE-CMR data and may permit the assessment of RV perfusion.

The potential of CMR to provide a comprehensive assessment of CAD has long been recognized. Cine and LGE-CMR are today considered gold standards for the assessment of contractile function and scar because of their high spatial resolution, tissue contrast, and diagnostic accuracy.[8–11] Despite similar image properties and theoretical advantages over competing imaging modalities, myocardial perfusion-CMR has been less enthusiastically embraced in clinical practice. The reasons for this include a lack of consistent acquisition protocols between vendors and institutions, lack of simple analysis tools and less consistent image quality. In addition, lower spatial resolution compared with cine and LGE-CMR and related limitations such as dark-banding artefacts have affected the use of perfusion-CMR in the past.[1–5]

This study demonstrates that adenosine stress perfusion-CMR at a spatial resolution similar to other CMR methods is achievable with 5× *k*–*t* SENSE acceleration. The high spatial resolution had several beneficial effects:

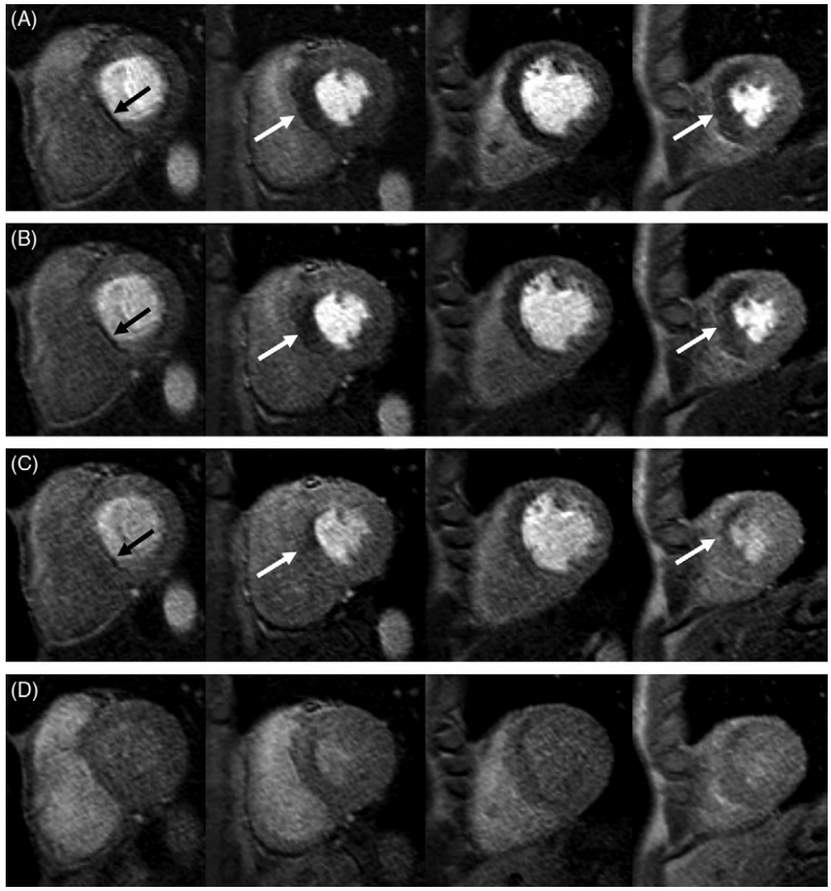

Figure 4 Case example: myocardial perfusion-cardiac magnetic resonance study of a 56-year-old patient with 90% stenosis of the left anterior descending coronary artery on subsequent coronary angiography. Four slices were acquired from the base (left) to the apex (right) and images at four time points during the contrast passage are shown from (*A*) to (*D*). In (*A*) and (*B*) images acquired in the early part of myocardial enhancement reveal a transmural perfusion defect, which becomes subendocardial in the washout phase of the contrast passage in (*C*) and (*D*). The left column shows a typical dark-banding artefact at the inferior septum. This artefact is most pronounced early during the contrast passage, reduces rapidly during contrast uptake in the myocardium, and in line with the high spatial resolution has a small transmural extent.

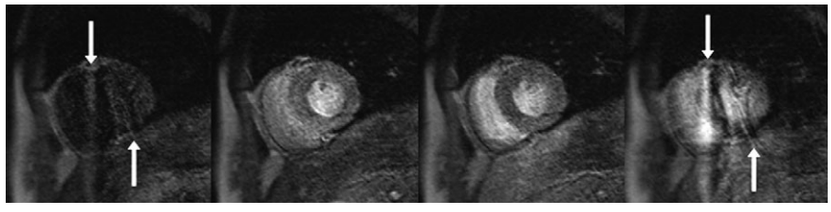

Figure 5 Respiratory and *k*–*t* reconstruction-related artefact: perfusion-cardiac magnetic resonance images from a patient who was unable to hold his breath during the stress-perfusion acquisition. Images from left to right show dynamic images reconstructed for different time points of the acquisition. The first and last images show reconstruction errors due to respiratory motion, whilst images during the myocardial contrast passage are relatively free of artefact, allowing an assessment of myocardial perfusion as normal.

First, the image quality of the high-resolution data was high as the image examples illustrate and only 2 of 54 studies were considered non-diagnostic. Subendocardial dark rim artefacts were small,[18,19] as demonstrated in *Figure 4*, and their diagnostic impact was minimal. Observer agreement was high for overall as well as segmental analysis.

Secondly, perfusion-CMR data could be directly correlated to cine and LGE-CMR data. Although the correlation of different components of a CMR study does not depend on their resolution alone, but also on acquiring data in the same spatial orientation, similar spatial resolution between the components facilitates, in particular, the analysis of patients with complex cardiovascular disease and previous myocardial infarction as shown in *Figure 3*. LGE-CMR is increasingly used for viability assessment in patients with known CAD, and the diagnostic value of CMR will be enhanced if other CMR components match in both spatial orientation as well as resolution.

Thirdly, the transmural extent of perfusion and its evolution over time were clearly delineated, as *Figure 4* shows. The transmural ischaemia gradient seen between multiple cardiac layers provided an additional marker of ischaemia, which was helpful in particular in detecting multi-vessel disease. Conventionally the visual analysis of perfusion-CMR data requires comparison with a normally perfused reference segment. This dependence on an intra-patient comparison is often regarded as an important impediment of visual analysis compared with semi-quantitative[3,5] and quantitative[20] analysis methods, in particular for the detection of balanced ischaemia in multi-vessel disease. Adding the transmural ischaemia distribution as a diagnostic marker of ischaemia in this study resulted in a similar diagnostic accuracy for detection of multi-vessel disease as for single vessel disease and may represent an important improvement of visual analysis of perfusion-CMR studies. However, this study has not shown a better diagnostic performance of high resolution perfusion-CMR compared with the published literature with previous methods and lower spatial resolution. A comparative study is needed to determine whether higher spatial resolution perfusion-CMR translates into improved diagnostic yield.

Recently, perfusion-CMR at 3 Tesla has been described with promising initial results.[21] *k*–*t* SENSE can be applied irrespective of the field strength and the SNR increase at 3 Tesla will partly compensate for the loss of SNR associated with higher spatial resolution and spatiotemporal undersampling. *k*–*t* SENSE accelerated perfusion-CMR at 3 Tesla is thus an attractive prospect.

This study also showed for the first time that perfusion-CMR has the potential to delineate RV ischaemia. Because the normal RV free wall is very thin, the visualization of its blood supply is challenging. Other diagnostic tests, in particular nuclear scintigraphy and echocardiography, are faced with similar challenges.[22,23] As shown, the high spatial resolution achieved in this work potentially allows the detection of RV ischaemia with perfusion-CMR, although our data are clearly preliminary and the number of patients with RV ischaemia ($n = 5$) was too small to draw firm conclusions. The main reason why RV perfusion could not be evaluated in one-third of patients was contrast agent persistence or recirculation into the RV cavity at the time of myocardial perfusion. Modifications of the contrast dose or injection speed might be necessary to optimize assessment of RV perfusion.

Data in this study were analysed at three stenosis levels of 50, 70, and 75% to permit a comparison with previous studies in which different cut-off levels were used to define significant stenosis. Reassuringly, the overall diagnostic performance of perfusion-CMR was similar at all stenosis severities, although CIs were wide given the small sample size.

As in the previous volunteer study,[14] data acquisition in this work was limited to systole and diastole with four slices acquired over two heartbeats. The motivation for limiting data acquisition to mid-systole and mid-diastole was to minimize artefacts related to cardiac motion and thus permit a more confident identification of potential artefacts related to the new method itself. It needs to be emphasized that the decision was entirely independent of the evaluation of the *k*–*t* SENSE method. Although it would have been possible to acquire additional slices, given the shot duration of 120 ms, the diagnostic accuracy of perfusion-CMR studies is not enhanced by acquiring additional slices in particular if they fall into phases of the cardiac cycle with rapid motion.[4,24] In order to compensate for the lower temporal resolution of acquisition at alternate heartbeats, we used a relatively high contrast medium dose of 0.1 mmol/kg compared with previous studies so that the wash-in phase was considerably prolonged. As illustrated in *Figure 4*, with this approach ischaemia persisted for several dynamic images.

Limitations

Like the majority of previous perfusion-CMR studies, we used X-ray coronary angiography to determine the presence of significant coronary stenosis. Due to local clinical management, invasive functional assessment of coronary stenoses was not available for all patients. Although the limitations of the X-ray angiogram to determine the functional significance of borderline coronary stenosis are well documented, it remains the most important clinical test to determine the need for revascularization in the real world.

k–*t* SENSE adds complexity to the acquisition of perfusion-CMR data. In particular, the method is sensitive to respiratory motion and cardiac arrhythmia. In this study, respiratory motion during data acquisition was found to affect not only the image frame(s) experiencing motion but also frames neighbouring in time (*Figure 5*). This observation relates to the periodicity assumed in the *k*–*t* SENSE reconstruction. However, breathing typically occurred towards the end of the acquisition and thus affected the last and first image frames, while data acquired during the myocardial contrast passage were generally artefact-free. Importantly, in our unselected clinical population only two patients (4%) had to be excluded from analysis because artefacts affected the myocardial contrast passage.

Conclusions

High spatial resolution perfusion-CMR is feasible in a clinical population. It accurately detects coronary artery stenosis in single and multi-vessel CAD, minimizes artefacts, and shows potential for an assessment of RV ischaemia. High spatial resolution perfusion-CMR may also provide an improved tool for the evaluation of conditions or therapies that predominantly affect subendocardial perfusion.

Acknowledgements

The authors thank Bayer Schering Pharma AG for providing the contrast agent.

Conflict of interest: none declared.

Funding

The authors thank Bayer Schering Pharma AG for financial support. This work was supported by Philips Medical Systems, Best, The Netherlands, and a Wellcome Trust fellowship to S.P.

Funding to pay the Open Access publication charges for this article was provided by the Wellcome Trust.

References

1. Wilke N, Jerosch-Herold M, Zenovich A, Stillman AE. Magnetic resonance first pass myocardial perfusion imaging: clinical validation and future applications. *J Magn Reson Imaging* 1999;**10**:676–685.
2. Al-Saadi N, Nagel E, Gross M, Bornstedt A, Schnackenburg B, Klein C, Klimek W, Oswald H, Fleck E. Noninvasive detection of myocardial ischemia from perfusion reserve based on cardiovascular magnetic resonance. *Circulation* 2000;**101**:1379–1383.
3. Schwitter J, Nanz D, Kneifel S, Bertschinger K, Büchi M, Knüsel PR, Marincek B, Lüscher TF, von Schulthess GK. Assessment of myocardial perfusion in coronary artery disease by magnetic resonance: a comparison with positron emission tomography and coronary angiography. *Circulation* 2001;**103**:2230–2235.
4. Nagel E, Klein C, Paetsch I, Hettwer S, Schnackenburg B, Wegscheider K, Fleck E. Magnetic resonance perfusion measurement for the noninvasive detection of coronary artery disease. *Circulation* 2003;**108**:432–437.
5. Giang TH, Nanz D, Coulden R, Friedrich M, Graves M, Al-Saadi N, Luscher TF, von Schulthess GK, Schwitter J. Detection of coronary artery disease by magnetic resonance myocardial perfusion imaging with various contrast medium doses: first European multi-centre experience. *Eur Heart J* 2004;**25**:1657–1665.
6. Plein S, Greenwood JP, Ridgway JP, Cranny G, Ball SG, Sivananthan MU. Assessment of non-ST-segment elevation acute coronary syndromes with cardiac magnetic resonance imaging. *J Am Coll Cardiol* 2004;**44**:2173–2181.
7. Bodi V, Sanchis J, Lopez-Lereu MP, Losada A, Nunez J, Pellicer M, Bertomeu V, Chorro FJ, Llacer A. Usefulness of a comprehensive cardiovascular magnetic resonance imaging assessment for predicting recovery of left ventricular wall motion in the setting of myocardial stunning. *J Am Coll Cardiol* 2005;**46**:1747–1752.
8. Kim RJ, Wu E, Rafael A, Chen EL, Parker MA, Simonetti O, Klocke FJ, Bonow RO, Judd RM. The use of contrast-enhanced magnetic resonance imaging to identify reversible myocardial dysfunction. *N Engl J Med* 2000;**343**:1445–1453.
9. Klein C, Nekolla SG, Bengel FM, Momose M, Sammer A, Haas F, Schnackenburg B, Delius W, Mudra H, Wolfram D, Schwaiger M. Assessment of myocardial viability with contrast-enhanced magnetic resonance imaging: comparison with positron emission tomography. *Circulation* 2002;**105**:162–167.
10. Myerson SG, Bellenger NG, Pennell DJ. Assessment of left ventricular mass by cardiovascular magnetic resonance. *Hypertension* 2002;**39**:750–755.
11. Alfakih K, Plein S, Thiele H, Jones T, Ridgway JP, Sivananthan MU. Normal human left and right ventricular dimensions for MRI as assessed by turbo gradient echo and steady-state free precession imaging sequences. *J Magn Reson Imaging* 2003;**17**:323–329.
12. Kellman P, Derbyshire JA, Agyeman KO, McVeigh ER, Arai AE. Extended coverage first-pass perfusion imaging using slice-interleaved TSENSE. *Magn Reson Med* 2004;**51**:200–204.
13. Tsao J, Boesiger P, Pruessmann KP. *k-t* BLAST and *k-t* SENSE: dynamic MRI with high frame rate exploiting spatiotemporal correlations. *Magn Reson Med* 2003;**50**:1031–1042.
14. Plein S, Ryf S, Schwitter J, Radjenovic A, Boesiger P, Kozerke S. Dynamic contrast-enhanced myocardial perfusion MR imaging accelerated with *k-t* SENSE. *Magn Reson Med* 2007;**58**:777–785.
15. Cerqueira MD, Weissman NJ, Dilsizian V, Jacobs AK, Kaul S, Laskey WK, Pennell DJ, Rumberger JA, Ryan T, Verani MS. Standardized myocardial segmentation and nomenclature for tomographic imaging of the heart: a statement for healthcare professionals from the Cardiac Imaging Committee of the Council on Clinical Cardiology of the American Heart Association. *Circulation* 2002;**105**:539–542.
16. Swets JA. Measuring the accuracy of diagnostic systems. *Science* 1988;**240**:1285–1288.
17. Bland JM, Altman DG. Statistical methods for assessing agreement between two methods of clinical measurement. *Lancet* 1986;**1**:307–311.
18. Di Bella EV, Parker DL, Sinusas AJ. On the dark rim artifact in dynamic contrast-enhanced MRI myocardial perfusion studies. *Magn Reson Med* 2005;**54**:1295–1299.
19. Storey P, Chen Q, Li W, Edelman RR, Prasad PV. Band artifacts due to bulk motion. *Magn Reson Med* 2002;**48**:1028–1036.
20. Jerosch-Herold M, Wilke N, Stillman AE. Magnetic resonance quantification of the myocardial perfusion reserve with a Fermi function model for constrained devolution. *Med Phys* 1998;**25**:73–84.
21. Cheng AS, Pegg TJ, Karamitsos TD, Searle N, Jerosch-Herold M, Choudhury RP, Banning AP, Neubauer S, Robson MD, Selvanayagam JB. Cardiovascular magnetic resonance perfusion imaging at 3-tesla for the detection of coronary artery disease: a comparison with 1.5-tesla. *J Am Coll Cardiol* 2007;**49**:2440–2449.
22. Chiba J, Takeishi Y, Abe S, Tomoike H. Visualisation of exercise-induced ischaemia of the right ventricle by thallium-201 single photon emission computed tomography. *Heart* 1997;**77**:40–45.
23. Inanir S, Dede F, Caliskan B, Erdil TY, Tokay S, Oktay A. Assessment of right and left ventricular perfusion in patients with right bundle branch block. *Arch Med Res* 2006;**37**:58–64.
24. Bertschinger KM, Nanz D, Buechi M, Luescher TF, Marincek B, von Schulthess GK, Schwitter J. Magnetic resonance myocardial first-pass perfusion imaging: parameter optimization for signal response and cardiac coverage. *J Magn Reson Imaging* 2001;**14**:556–562.

The above article uses a new reference style being piloted by the EHJ that shall soon be used for all articles.